Summer 7-15-2015

Numerical Analysis of Bubble Dynamics in Electrohydraulic and Electromagnetic Shock Wave Lithotripsy

Jun Qin
Southern Illinois University Carbondale, jqin@siu.edu

Recommended Citation
Qin, Jun. "Numerical Analysis of Bubble Dynamics in Electrohydraulic and Electromagnetic Shock Wave Lithotripsy." *International Journal of Computational Biology and Drug Design* 8, No. 2 (Summer 2015): 105-113. doi:10.1504/IJCBDD.2015.071126.

Numerical Analysis of Bubble Dynamics in Electrohydraulic and Electromagnetic Shock Wave Lithotripsy

Jun Qin

Department of Electrical and Computer Engineering
Southern Illinois University Carbondale
Mail Code 6603, 1230 Lincoln Drive,
Carbondale, IL 62901, USA
Email: jqin@siu.edu

Abstract: This study numerically investigated the bubble dynamics in electrohydraulic (EH) and electromagnetic (EM) shock wave lithotripsy (SWL). The acoustic pressure generated by a typical EH (i.e., Dornier HM-3) and EM (i.e., Siemens Modularis) lithotripters has been measured. The dynamics of cavitation bubbles in SWL has been numerically simulated using the Gilemore formulation coupled with zero-order gas diffusion. The pressure measurement results showed that both the peak positive and negative pressure of the Modularis at E4.0 are slightly higher than the corresponding values of the HM-3 at 20 kV. However, the pressure waveforms generated by an EH lithotripter is different from these of an EM lithotripter. The EM shock wave has a remarkable 2nd compressive pulse, which might suppress the cavitation activities in the EM lithotripter. In addition, the numerical simulation showed the EH lithotripter could produce stronger cavitation activities than the EM lithotripter.

Keywords: Shock wave lithotripsy, Cavitation bubble dynamics, Gilemore modeling Electrohydraulic and Electromagnetic lithotripsy

INTRODUCTION

Since introduced in early 1980s, shock wave lithotripsy (SWL) has rapidly emerged the primary treatment modality for kidney and upper urinary stone disease worldwide (Chaussy and Fuchs, 1989). The initial success of SWL prompted several manufacturers to introduce the newer generation lithotripters: 2nd generation SWL was introduced in the late 1980s (Lingeman *et al.*, 2003a; Zhong, 2007), and the 3rd generation lithotripters in early 1990s (Qin *et al.*, 2010). With the hope of improving overall performance and user convenience, the newer generation SWLs used different

technologies for generation of shock wave, wave focusing, acoustical coupling, stone localization, etc (Lingeman *et al.*, 2003a; Zhou *et al.*, 2004). Unfortunately, comparing to the original Dornier HM-3 lithotripter, the newer generation SWLs were found to be less effective on stone fragmentation yet with increased propensity for tissue injury and higher stone recurrent rate (Graber *et al.*, 2003; Lingeman *et al.*, 2003b; Gerber *et al.*, 2005a).

One major change in the design of the newer generation lithotripters is the replacement of electrohydraulic (EH) shock source by electromagnetic (EM) shock source. The Dornier HM-3 utilizes EH technology in the form of employing an underwater electrical spark discharge for shock wave generation and a truncated ellipsoidal reflector for wave focusing. The HM-3 requires electrode change within every 2000 shocks (i.e., one clinic treatment), and electrode cost was believed to be one of the reasons for replacing the EH shock source with the EM shock source in most of the 2nd and 3rd generation lithotripters (Lingeman *et al.*, 2003a). In a typical EM shock wave lithotripter, a capacitor is discharged rapidly through a coil to repel an adjacent thin metallic membrane, thus producing a plane wave with relatively low pressure. Subsequently, this plane wave focused by an acoustic lens or in the case of cylindrical coil systems through a parabolic reflector to generate a focused shock wave (Coleman and Saunders, 1993).

Comparing to EH lithotripters, the acoustic field generated by EM lithotripters is much more stable and highly reproducible (Lingeman *et al.*, 2003a). However, clinical experience and clinical studies in past decade have indicated that comminution efficiency with a concomitantly increased retreatment rate (EM lithotripters generally produce a lower), compared to the original HM-3 lithotripter (Graber *et al.*, 2003; Lingeman *et al.*, 2003a; Gerber *et al.*, 2005b). Although the underlying mechanism has not been completely understood, some key differences such as the changes of focal beam size (Qin *et al.*, 2010), pressure waveform profile (Leitao *et al.*, 2007), cavitation activity, and acoustical coupling (Cartledge *et al.*, 2001; Jain and Shah, 2007; Li *et al.*, 2012; Lautz *et al.*, 2013), may contribute to the decreased stone comminution produced by EM lithotripters.

In a lithotripter field, cavitation bubbles are produced by the negative pressure of the leading shock wave (LSW). These bubbles expand to several hundred times of their original size, and then collapse violently, generating strong secondary shock wave emission and high-speed jets impinging onto the stone surface. In this paper, we will theoretically investigate of cavitation activity produced by EH and EM SWLs based on the Gilemore formulation for bubble dynamics coupled with zero-order gas diffusion.

METHOD AND MATERIALS

1. Modeling of bubble dynamics in SWL

Several models have been developed for describing the dynamics of a spherical bubble oscillation in free field, including the Rayleigh-Plesset equation, the Herring-Trilling equation, and the Gilmore equation (Young, 1999). Church used the Gilmore formulation coupled with a zero-order model of gas diffusion to model the dynamics of a single spherical bubble generated in SWL (Church, 1989). Coleman and colleagues also used the Gilmore model to study the cavitation produced by the 1st and 2nd shock wave in an HM-3 lithotripter, and confirmed the theoretical results by measurement of acoustic emission signals (Coleman *et al.*, 1992). Ding and Gracewski proposed a modified Gilmore model, in which a viscoelastic membrane was included in the original Gilmore model, to model the dynamics of bubble with a viscoelastic wall (Ding and Gracewski, 1994). Zhu and Zhong used the Gilmore model coupled with zero-order gas diffusion to simulate the dynamics of bubble produced by different shock wave sequences of a modified XL-1lithotripter (Zhu and Zhong, 1999).

2. **Gilmore formulation for bubble dynamics**

The original Gilmore formation for bubble dynamics was used to simulate the oscillation of a spherical bubble in a lithotripter field (Zhu and Zhong, 1999).

$$R(1-\frac{U}{C})\frac{dU}{dt}+\frac{3}{2}\left(1-\frac{U}{3C}\right)U^2=(1+\frac{U}{C})H+\frac{1}{C}(1-\frac{U}{C})R\frac{dH}{dt} \tag{1}$$

where R is the bubble radius, U (= dR/dt) is the velocity of the bubble wall, C is the speed of sound in the liquid at the bubble wall, H is the enthalpy difference between the liquid at infinite pressure P_∞ and the pressure at bubble wall $P(R)$. H and C can be defined by

$$C=\left[C_l^2+(m-1)H\right]^{1/2} \tag{2}$$

where C_l is the infinitesimal speed of sound in the liquid and m is a constant.

$$H=\int_{P_\infty}^{P(R)}\frac{dP}{\rho} \tag{3}$$

where P and ρ are the time varying pressure and the density of the liquid respectively. The pressure P can be determined by the state equation of a compressible fluid, $P=A(\rho/\rho_0)^m-B$, where ρ_0 is the density of the equilibrium liquid, and $A=C_l^2\,\rho/P_0 m$ with $m=7$, and $B=A-1$. Further, the pressure at the bubble wall $P(R)$ was given by $P(R)=P_g-\frac{2\sigma}{R}-\frac{4\mu}{R}U$, where P_g is the gas pressure inside the bubble, μ is liquid viscosity and σ is the surface tension in the liquid. When a pressure

produced by a SWL $P_S(t)$ is far away from the bubble, it can be considered as $P_S(t) = P_\infty - P_0$, where P_0 is the ambient pressure of the surrounding liquid.

The gas diffusion across the bubble wall can be described by a diffusion equation for the concentration of gas dissolved in the liquid (Eller and Flynn, 1965):

$$\frac{dc}{dt} = \frac{\partial c}{\partial t} + v \cdot \nabla c = D\nabla^2 c \tag{4}$$

where c is the concentration of gas in the liquid, v and D are the velocity of the liquid and a diffusion constant respectively.

The instantaneous number of moles of gas n in a bubble can be calculated by using the zeroth-order solution to the gas diffusion equation:

$$n = n_0 - 4(\pi D)^{1/2} \int_0^\tau F\left(\tau^{'}\right)(\tau - \tau')^{1/2} d\tau' \tag{5}$$

where n_0 is the number of moles gas initially present in the bubble, and

$$\tau = \int_0^t R^4(t')dt' \tag{6}$$

$$F(\tau) = c_0(P_g / P_0) - c_l \tag{7}$$

where c_0 and c_l are the saturation concentration of the gas in the liquid and the initial concentration of gas in the liquid far from bubble respectively, and

$$P_g = \left(P_0 + \frac{2\sigma}{R_0}\right)\frac{n}{n_0}\left(\frac{R_0}{R}\right)^{3\eta}\left(\frac{R_{0n}}{R_0}\right)^{3(\eta-1)} \tag{8}$$

where R_0 is the initial equilibrium radius of the bubble, R_{0n} is the time-varying equilibrium bubble radius, η is the polytropic exponent of the gas.

3. **Numerical calculation**

For numerical calculations, the Gilmore formation (Eqn. 2.19) will be nondimensionalized, and solved by using the fifth-order Runge-Kutta-Fehlberg method with a step-size control algorithm (Zhu and Zhong, 1999). The values of the physical constants for water are $\rho_0 = 998kg/m^3$, $R_0 = 3\mu m$, $\mu = 1.046\times10^{-3} kg/m\cdot s$, $\sigma = 72.583\times10^{-3} N/m$, $C_l = 1500m/s$, $\eta = 1.4$, and $P_0 = 1.01\times10^5 Pa$. The maximum size R_{max} and the collapse time t_c of a bubble will be calculated by using the measured pressure data as $P_s(t)$.

4. Experimental measurement of shock wave

A. Lithotripters: EH (HM-3) and EM (Modularis)

In this study, the acoustical fields produced by a representative EH lithotripter (i.e., Unmodified Dornier HM-3) and an EM lithotripter (i.e., Siemens Modularis) were investigated and compared. The Dornier HM-3 uses EH source to generate shock waves and an ellipsoidal reflector for acoustic wave focusing. While the Siemens Modularis uses an EM source to generate shock wave, an acoustic lens for shock wave focusing, and a rubber balloon for coupling. For pressure measurement in the Modularis, the experiments were carried out in a specially constructed polycarbonate water tank attached to the shock head of the lithotripter.

B. Pressure measurement

The acoustic fields produced by the HM-3 and Modularis were measured by using a light spot hydrophone (LSHD-2, University of Erlangen-Nuremberg,, Germany). The optical head of the LSHD was attached to a 3D translation stage (Velmex, Bloomfield, NY), and aligned vertically to the lithotripter axis. Accurate alignment of the LSHD at the focus point F_2 was aided by a mechanical pointer. Ten pressure waveforms were recorded using a digital oscilloscope (LeCroy 9314M, Chestnut ridge, NY) operated at a 100-MHz sampling rate. The oscilloscope was triggered by the light emitted from the spark discharge of the HM-3 lithotripter or the electromagnetic spike from the condenser discharge off the Modularis lithotripter.

RESULTS AND DISCUSSION

Pressure waveforms of LSW in the EH and EM Lithotripters

Figure 1 shows two representative pressure waveforms of the LSW at the focus produced by the HM-3 at 20 kV and Modularis at E4.0, respectively. Both the peak positive (p_+ = 49.8 ± 1.8 MPa) and peak negative (p_- = -10.7 ± 1.4 MPa) pressure of the HM-3 are slightly lower than the corresponding values of the Modularis (p_+ = 52.3 ± 2.1 MPa) and (p_- = -13.4 ± 3.4 MPa).

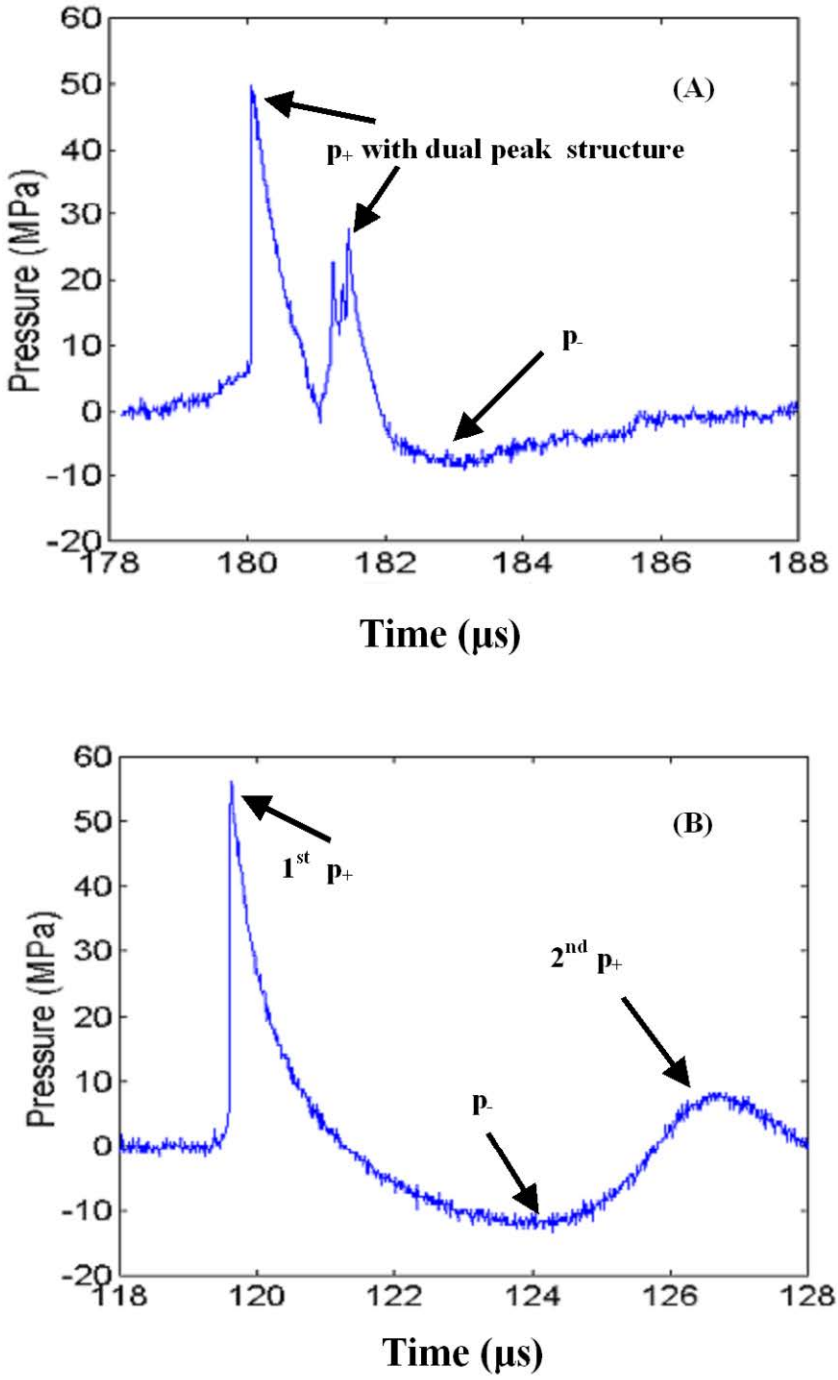

Figure 1: Representative pressure waveforms at the lithotripter focus produced by (A) the HM-3 at 20 kV and (B) Modularis at E4.0.

In addition, several notable differences can be observed in two waveforms. In the HM-3 at 20 kV, a typical LSW arrives at F_2 in about 180 μs after the spark discharge (Figure 1A). The waveform consists of a leading compressive wave with ~ 2 μs zero-crossing pulse duration and a dual-peak structure, followed by a tensile component of ~ 4 μs pulse duration.

In comparison, the LSW produced by the Modularis at E4.0 arrives at ~119 μs after the condenser discharge of the Modularis (Figure 1B). The waveform is led by a single compressive component of ~ 1 μs pulse duration followed by a tensile wave with ~ 4 μs pulse duration, which is further followed by a 2nd compressive pulse with low peak positive pressure. The remarkable 2nd compressive pulse in the EM lithotripter may suppress the cavitation activities. Similar features have been reported in previous studies for EM lithotripters (Coleman and Saunders, 1989; Eisenmenger, 2001; Eisenmenger *et al.*, 2002).

Assessment of cavitation by the Gilmore Model

The Gilmore model with the zero-gas diffusion was used to simulate the dynamic of single cavitation bubbles produced in the lithotripter field. The pressure waveforms measured at F_2 in the HM-3 at 20 kV and the Modularis at E4.0 were used as the input in the Gilmore model calculation.

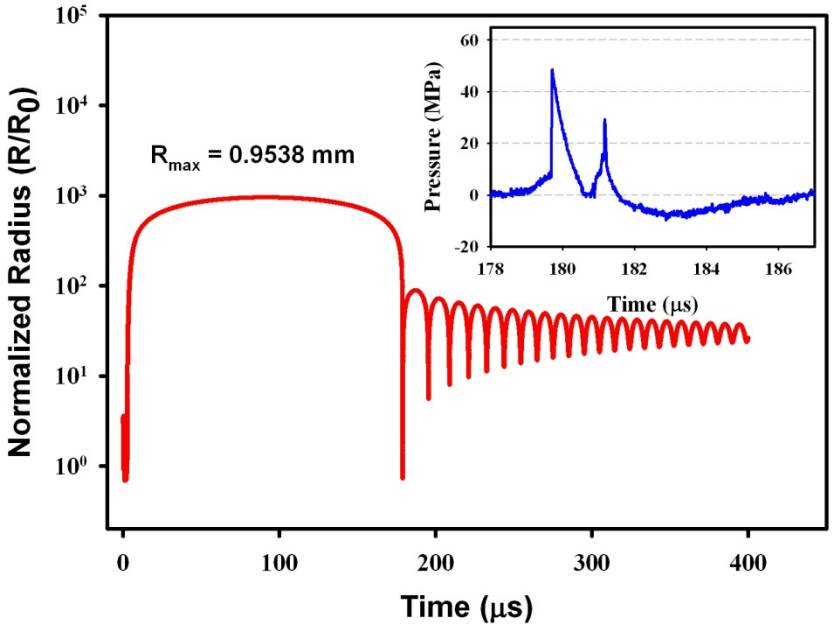

Figure 2: Theoretical calculation of bubble dynamics by using Gilmore model with a measured LSW (inserted figure) produced at *F2* by the HM-3 at 20 kV.

Figure 2 shows a calculated bubble response to a pressure waveform measured at F_2 in the HM-3 at 20 kV (the waveform is shown in the inset in Figure 2). In response to the compressive component in LSW, the bubble was first collapsed, and then expanded quickly and reached to a maximum bubble radius of 0.95 mm, which is about 300 times of its initial radius $R_0 = 3\mu m$.

Subsequently, the bubble collapsed violently at about 180 μs, and then subsequently growth and collapse cycles.

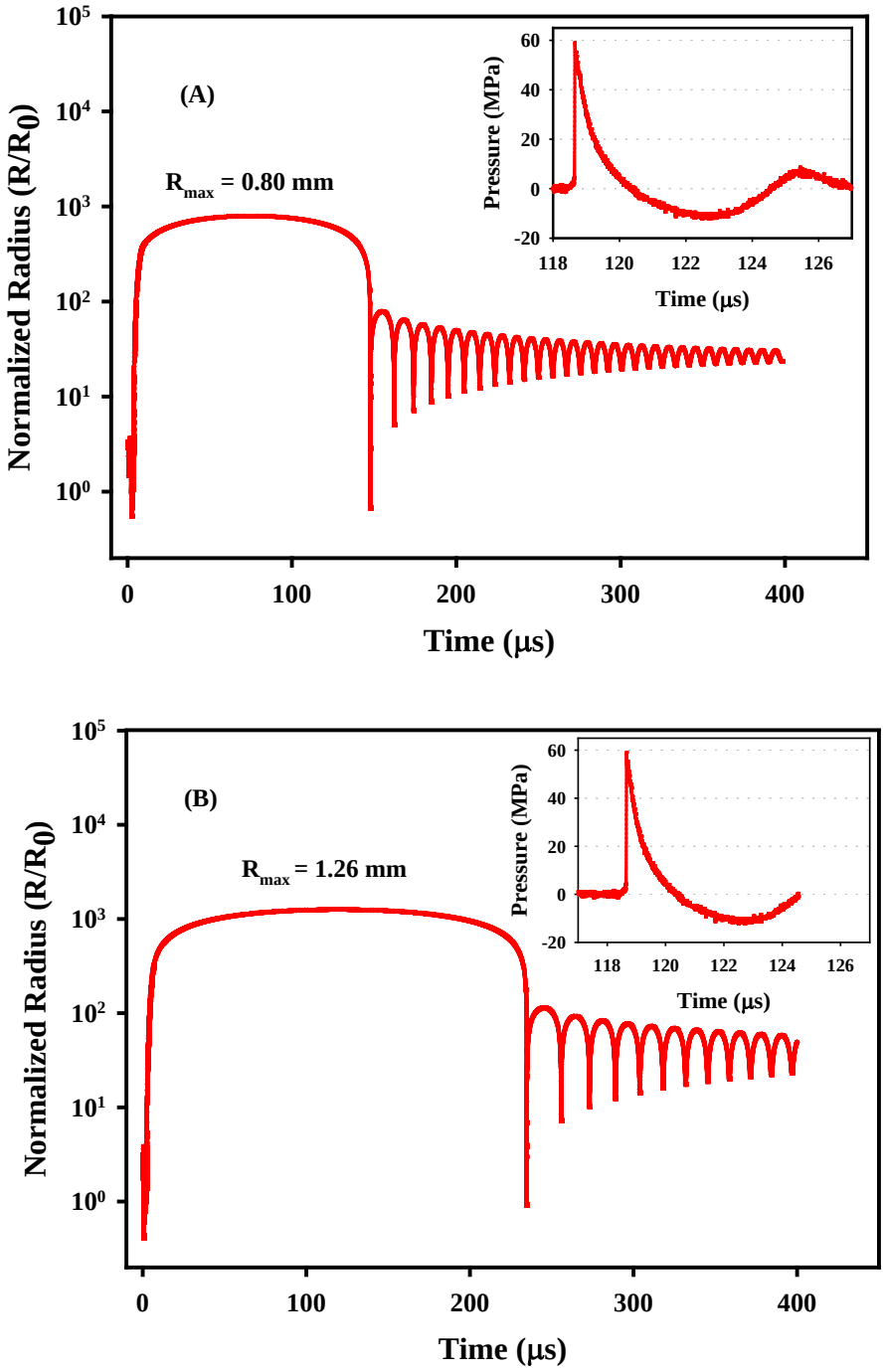

Figure 3:Theoretical calculations of the bubble dynamics by using a measured LSW (inserted figures) produced at F_2 by the Modularis at E4.0, with (A) including 2nd compressive component, and (B) excluding 2nd compressive component.

Figure 3 shows two model calculation results based on one LSW measured at F_2 in the Modularis at E4.0. The first bubble response (in Figure 3A) was calculated by using the entire waveform from 118 to 127 μs, which includes the 1st compressive, tensile wave, and 2nd compressive pulses (see the inset in Figure 3A). The maximum bubble radius is found to be 0.8 mm, which is smaller than it of the HM-3 at 20 kV. The bubble collapse time is also shorter than the value of HM-3. This result suggests the cavitation activities produced by the Modularis at E4.0 are weaker than these produced by the HM-3 at 20 kV.

However, in the second calculation, a truncated waveform was used, and the calculation time is from 118 to 124.6 μs, which is not including the 2nd compressive wave (see the inset in Figure 3B). The maximum bubble radius is found to be 1.2 mm, which is significantly larger than the corresponding values in the first calculation, as well as of the HM-3 at 20 kV. These results indicate that the 2nd compressive pulse in the EM lithotripter could significantly suppress the expansion of bubble, and therefore, influence the stone comminution in SWL.

Cavitation bubble in a lithotripter field is determined predominately by the tensile component of the LSW (Church, 1989; Choi *et al.*, 1993). The Modularis at E4.0 was found to produce higher peak negative pressure than the HM-3 at 20 kV, and the time duration of tensile components in both waveforms are comparable. Therefore, stronger cavitation activities were expected to produce by the Modularis. However, the theoretical calculation results have shown the significant reduction of the maximum bubble radius due to the 2nd compressive pulse in an EM shock wave. So this 2nd compressive pulse might suppress the cavitation in the EM lithotripter, and thus reduce stone comminution.

CONCLUSION

In this study, the acoustic pressure produced by EH and EM SWLs were measured. The waveforms of two SWLs were found to be different. In addition, the bubble dynamics was numerically simulated using the Gilemore formulation, and the results showed the EH lithotripter could produce stronger cavitation activities than the EM lithotripter. The results also indicated the remarkable 2nd compressive pulse, which is unique in the EM lithotripter, might suppress the cavitation activities.

REFERENCES

Cartledge, J. J., Cross, W. R., Lloyd, S. N., and Joyce, A. D. (**2001**). "The efficacy of a range of contact media as coupling agents in extracorporeal shockwave lithotripsy," BJU International **88**, 321-324.

Chaussy, C., and Fuchs, G. J. (**1989**). "Current state and future developments of noninvasive treatment of human urinary stones with extracorporeal shock wave lithotripsy," J. Urol. **141**, 782-792.

Choi, M. J., Coleman, A. J., and Saunders, J. E. (**1993**). "The influence of fluid properties and pulse amplitude on bubble dynamics in the field of a shock-wave lithotripter," Phys. in Med. & Biol. **38**, 1561-1573.

Church, C. C. (**1989**). "A Theoretical-Study of Cavitation Generated by an Extracorporeal Shock-Wave Lithotripter," J. Acoust. Soc. Am. **86**, 215-227.

Coleman, A. J., Choi, M. J., Saunders, J. E., and Leighton, T. G. (**1992**). "Acoustic emission and sonoluminescence due to cavitation at the beam focus of an electrohydraulic shock wave lithotripter," Ultrasound Med. Biol. **18**, 267-281.

Coleman, A. J., and Saunders, J. E. (**1989**). "A survey of the acoustic output of commercial extracorporeal shock wave lithotripters," Ultrasound Med. Biol. **15**, 213-227.

Coleman, A. J., and Saunders, J. E. (**1993**). "A review of the physical properties and biological effects of the high amplitude acoustic fields used in extracorporeal lithotripsy," Ultrasonics **31**, 75-89.

Ding, Z., and Gracewski, S. M. (**1994**). "Response of constrained and unconstrained bubbles to lithotripter shock wave pulses," J. Acoust. Soc. Am. **96**, 3636-3644.

Eisenmenger, W. (**2001**). "The mechanisms of stone fragmentation in ESWL," Ultrasound Med. Biol. **27**, 683-693.

Eisenmenger, W., Du, X. X., Tang, C., Zhao, S., Wang, Y., Rong, F., Dai, D., Guan, M., and Qi, A. (**2002**). "The first clinical results of "wide-focus and low-pressure" ESWL," Ultrasound Med. Biol. **28**, 769-774.

Eller, A., and Flynn, H. G. (**1965**). "Rectified Diffusion during Nonlinear Pulsations of Cavitation Bubbles," The Journal of the Acoustical Society of America **37**, 493-503.

Gerber, R., Studer, U. E., and Danuser, H. (**2005a**). "Is newer always better? A comparative study of 3 lithotriptor generations," J. Urol. **173**, 2013-2016.

Gerber, R., Studer, U. E., and Danuser, H. (**2005b**). "Is newer always better? A comparative study of 3 lithotriptor generations," J. Urol. **173**, 2013-2016.

Graber, S. F., Danuser, H., Hochreiter, W. W., and Studer, U. E. (**2003**). "A prospective randomized trial comparing 2 lithotriptors for stone disintegration and induced renal trauma," J. Urol. **169**, 54-57.

Jain, A., and Shah, T. K. (**2007**). "Effect of air bubbles in the coupling medium on efficacy of extracorporeal shock wave lithotripsy," European Urology **51**, 1680-1687.

Lautz, J., Sankin, G., and Zhong, P. (**2013**). "Turbulent water coupling in shock wave lithotripsy," Physics in Medicine and Biology **58**, 735-748.

Leitao, V. A., Simmons, W. N., Zhou, Y. F., Qin, J., Cocks, F. H., Fehre, J., Granz, B., Nanke, R., Preminger, G. M., and Zhong, P. (**2007**). "In vitro comparison between HM-3 and MODULARIS lithotripters," in *Renal Stone Disease*, edited by A. P. Evan, J. E. Lingeman, and J. C. Williams, pp. 372-376.

Li, G., Williams, J. C., Jr., Pishchalnikov, Y. A., Liu, Z., and McAteer, J. A. (**2012**). "Size and location of defects at the coupling interface affect lithotripter performance," Bju International **110**, E871-E877.

Lingeman, J. E., Kim, S. C., Kuo, R. L., McAteer, J. A., and Evan, A. P. (**2003a**). "Shockwave lithotripsy: Anecdotes and insights," J. Endourol. **17**, 687-693.

Lingeman, J. E., Kim, S. C., Kuo, R. L., McAteer, J. A., and Evan, A. P. (**2003b**). "Shockwave lithotripsy: Anecdotes and insigts," J. Endourol. **17**, 687.

Qin, J., Simmons, W. N., Sankin, G., and Zhong, P. (**2010**). "Effect of lithotripter focal width on stone comminution in shock wave lithotripsy," J. Acoust. Soc. Am. **127**, 2635-2645.

Young, F. R. (**1999**). "Cavitation- Bubble Dynamics," Imprial College Press, 8-37.

Zhong, P. (**2007**). "Innovations in lithotripsy technology," in *AIP Conference Proceedings* (Indianapolis, IN), pp. 317-325.

Zhou, Y. F., Cocks, F. H., Preminger, G. M., and Zhong, P. (**2004**). "Innovations in shock wave lithotripsy technology: Updates in experimental studies," J. Urol. **172**, 1892-1898.

Zhu, S. L., and Zhong, P. (**1999**). "Shock wave-inertial microbubble interaction: A theoretical study based on the Gilmore formulation for bubble dynamics," J. Acoust. Soc. Am. **106**, 3024-3033.